Wilting_Supplemental Figure 1

A

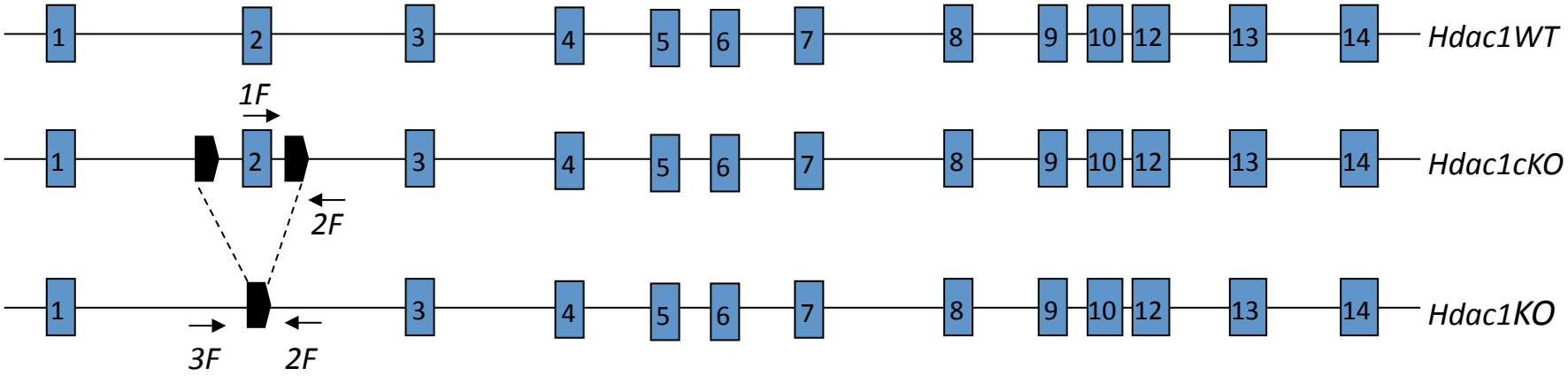

B

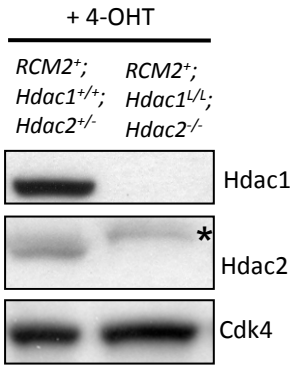

Wilting_Supplemental Figure 2

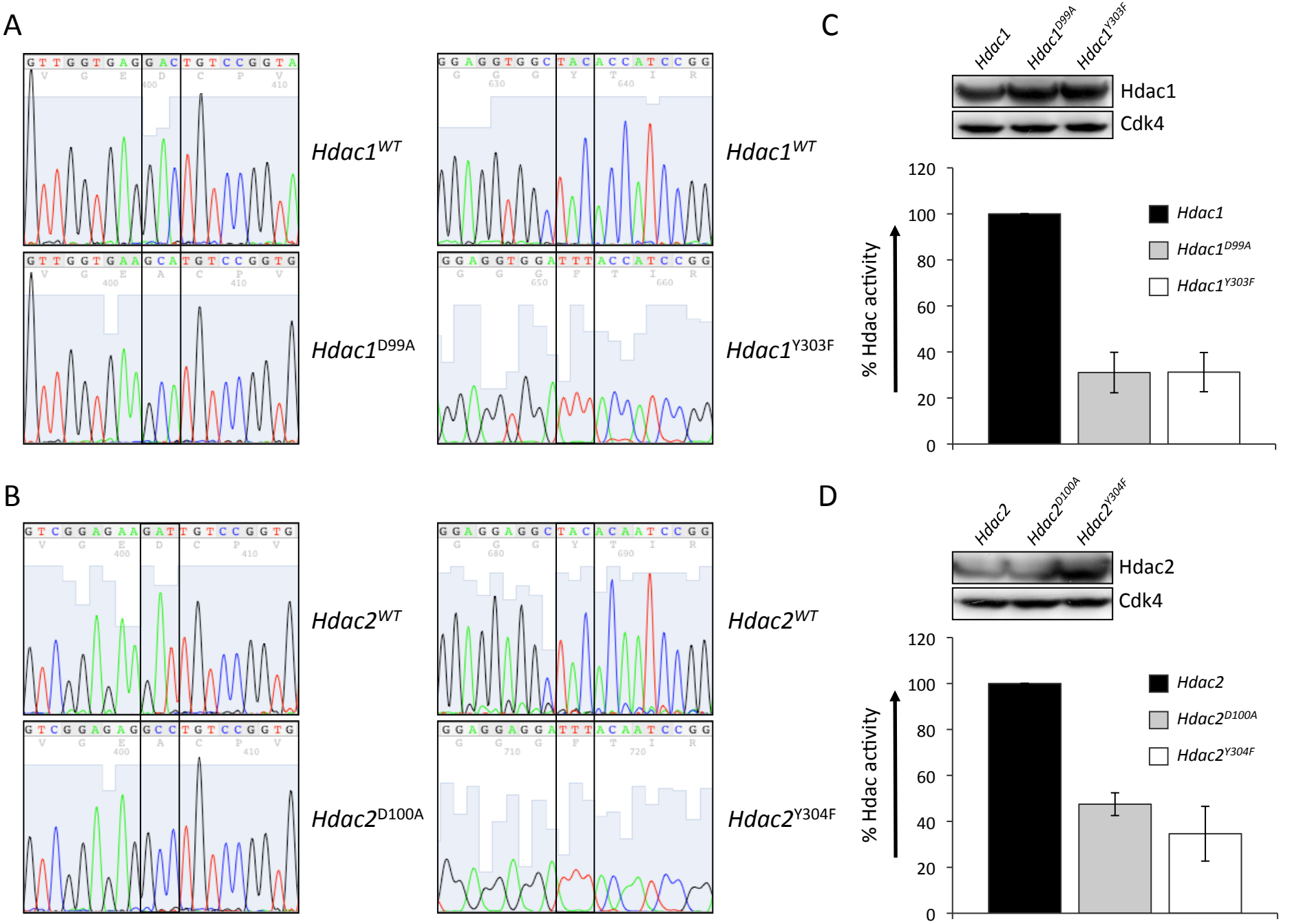

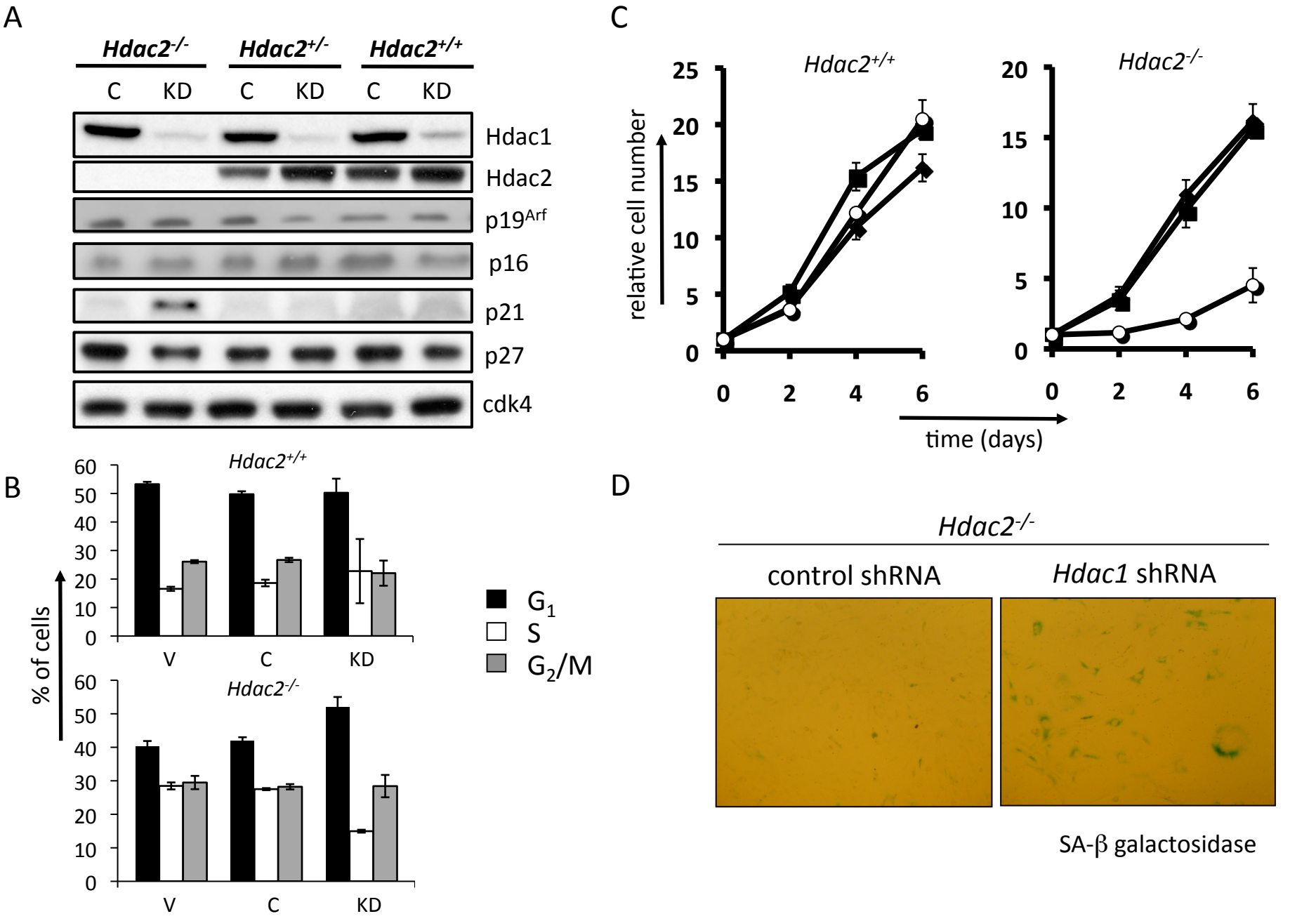
A
Hdac2-/-
Hdac2+/-
Hdac2+/+
C
KD
C
KD
C
KD
Hdac1
Hdac2
p19Arf
p16
p21
p27
cdk4
B
Hdac2+/+
Hdac2-/-
% of cells
60
50
40
30
20
10
0
V
C
KD
G1
S
G2/M
C
Hdac2+/+
Hdac2-/-
relative cell number
25
20
15
10
5
0
0
2
4
6
time (days)
D
Hdac2-/-
control shRNA
Hdac1 shRNA
SA-β galactosidase

Wilting_Supplemental Figure 4

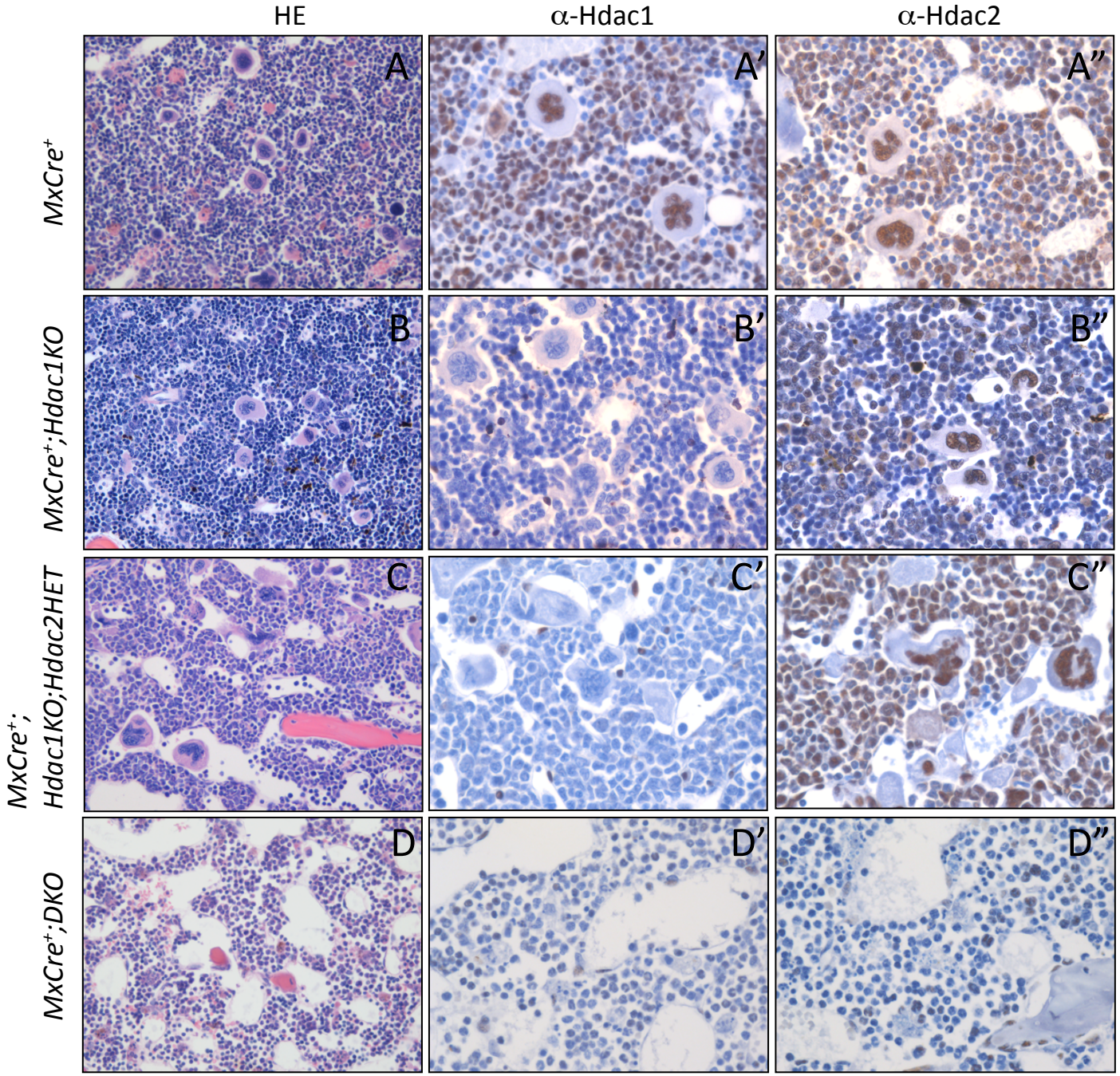

Wilting_Supplemental Figure 5

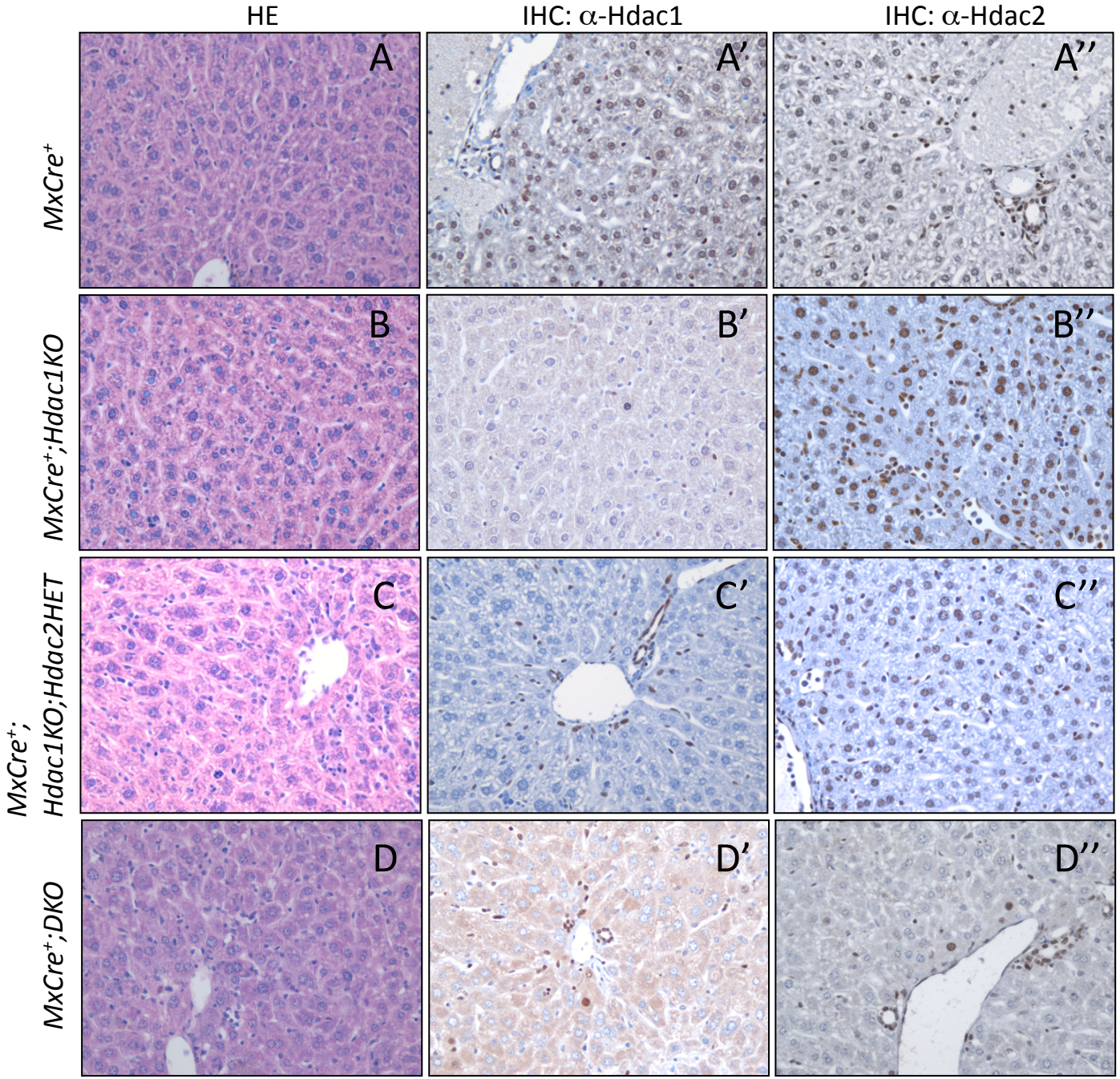

Wilting_Supplemental Figure 6

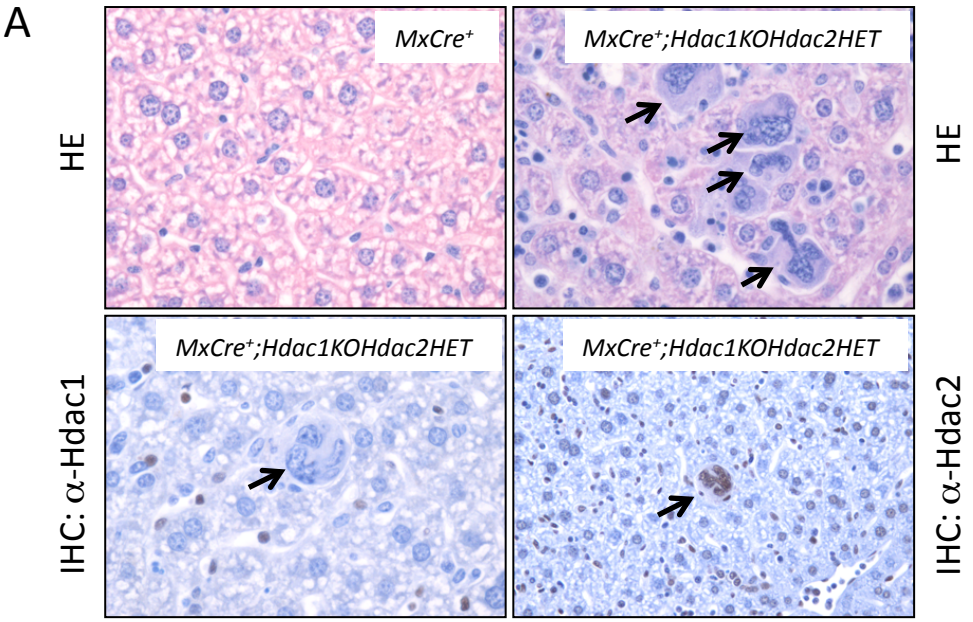

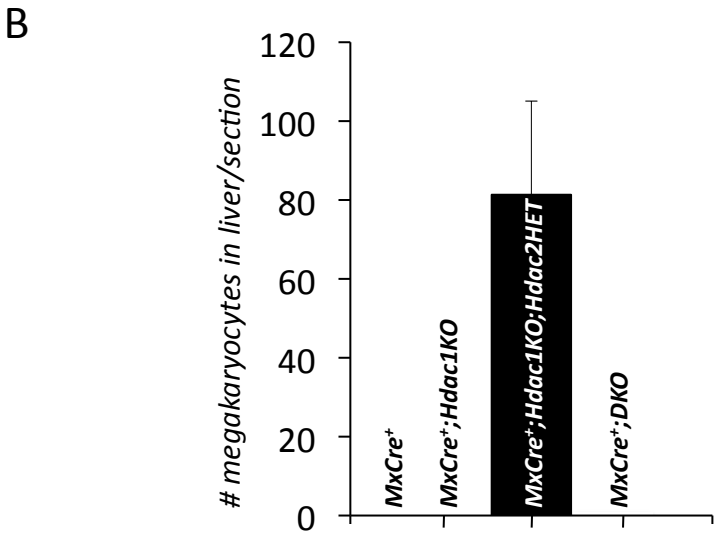

Legends of supplementary figures.

Supplemental Figure 1. A. Schematic representation of wild-type (*Hdac1WT*), conditional knock-out (*Hdac1cKO*) and null-allele (*Hdac1KO*) of Hdac1. Black arrow heads indicate the position of *loxP* sequences. Arrows indicate primers used for genotype purposes. B. Western blot analysis of protein lysates from tamoxifen (4-OHT) treated (200 nM) $RCM2^{+};Hdac1^{L/+};Hdac2^{+/-}$ and $RCM2^{+};Hdac1^{L/L};Hdac2^{-/-}$ MEFs. Asterix indicates a background signal, which becomes visible only in the absence of Hdac2.

Supplemental Figure 2. A. Sequence analysis of wild-type Hdac1 and $Hdac1^{D99A}$ and $Hdac1^{Y303F}$ mutants B. Sequence analysis of wild-type Hdac2 and $Hdac2^{D100A}$ and $Hdac1^{Y304F}$ mutants. Boxed areas indicate the amino acid substitution in the Hdac1 and Hdac2 mutants. C/D. Hdac activity of wild-type and mutant Hdac1 (C) or Hdac2 (D) as measured by incubating immunoprecipitated wild-type and mutant Hdac1 or Hdac2 with a fluorigenic acetylated substrate. Hdac activity is presented as percentage activity relative to the Hdac activity of wild-type Hdac1 and Hdac2. Hdac1 and Hdac2 western blot analysis of 293T total cell lysates containing wild-type or mutant Hdac1 or Hdac2, as used for immunoprecipitation. Cdk4 served as a loading control.

Supplemental Figure 3. A. Westernblot analysis of protein lysates of $Hdac2^{+/+}$, $Hdac2^{+/-}$ and $Hdac2^{-/-}$ MEFs expressing either control shRNA or *Hdac1* shRNA. Note the up regulation of Hdac2 upon knockdown of Hdac1. Cdk4 was used as loading control. B. Cell cycle analysis of $Hdac2^{+/+}$ and $Hdac2^{-/-}$ MEFs expressing empty vector (V), a control shRNA (C) or *Hdac1* shRNA (KD) using BrdU-PI FACS. C. Growth curve analysis of $Hdac2^{+/+}$ and $Hdac2^{-/-}$ MEFs expressing either empty vector (squares), control shRNA (diamonds) and *Hdac1* shRNA (open circles). D. Senescence-associated β-galactosidase staining of $Hdac2^{-/-}$ MEFs expressing either control shRNA or *Hdac1* shRNA.

Supplemental Figure 4. Representative photographs of hematoxylin-eosin stained bone-marrow sections of $MxCre^{+}$ (A), $MxCre^{+};Hdac1KO$ (B) and $MxCre^{+};Hdac1KO;Hdac2HET$ (C) and $MxCre^{+};DKO$ (D) mice. Immunohistochemistry using antibodies against Hdac1 (A'-D') and Hdac2 (A''-D'')

reveals efficient deletion of Hdac1 in bone marrow of *MxCre*$^{+}$*;Hdac1KO* and *MxCre*$^{+}$*;Hdac1KO;Hdac2HET* mice and efficient deletion of Hdac2 in bone marrow of *MxCre*$^{+}$*;DKO* mice.

Supplemental Figure 5. Representative photographs of hematoxylin-eosin stained liver sections of *MxCre*$^{+}$(A), *MxCre*$^{+}$*;Hdac1KO* (B) and *MxCre*$^{+}$*;Hdac1KO;Hdac2HET* (C) and *MxCre*$^{+}$*;DKO* (D) mice. Immunohistochemistry using antibodies against Hdac1 (A'-D') and Hdac2 (A''-D'') reveals efficient deletion of Hdac1 in liver of *MxCre*$^{+}$*;Hdac1KO* and *MxCre*$^{+}$*;Hdac1KO;Hdac2HET* mice and efficient deletion of Hdac2 in liver of *MxCre*$^{+}$*;DKO* mice.

Supplemental Figure 6. A. Representative photographs of hematoxylin-eosin or α-Hdac1 and α-Hdac2 stained liver sections of *MxCre*$^{+}$ and *MxCre*$^{+}$*;Hdac1KO;Hdac2HET* mice. Arrows indicate megakaryocytes. B. Average megakaryocyte counts in *MxCre*$^{+}$, *MxCre*$^{+}$*;Hdac1KO*, *MxCre*$^{+}$*;Hdac1KO;Hdac2HET* and *MxCre*$^{+}$*;DKO* liver as counted in liver sections of 3 independent mice of each genotype.